Safe optimal control of cancer using a Control Barrier Function technique

Ahmadi, Zahra; Razminia, Abolhassan

Published in:
Mathematical Biosciences

DOI:
10.1016/j.mbs.2024.109142

Published: 01/03/2024

Document Version
Final published version

Document License
CC BY

Mathematical Biosciences 369 (2024) 109142

Contents lists available at ScienceDirect

Mathematical Biosciences

journal homepage: www.elsevier.com/locate/mbs

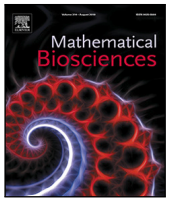

Original Research Article

Safe optimal control of cancer using a Control Barrier Function technique

Zahra Ahmadi [a], Abolhassan Razminia [a,b,*]

[a] Department of Electrical Engineering, Faculty of Intelligent Systems Engineering and Data Science, Persian Gulf University, Bushehr, Iran
[b] Process Control Laboratory, Faculty of Natural Sciences and Engineering, Åbo Akademi University, Turku, Finland

ARTICLE INFO

Keywords:
Optimal control
Control Barrier Function
Cancer therapy
Safety constraints
Tumor reduction

ABSTRACT

This paper addresses the problem of designing a safe and optimal control strategy for typical cancer using the Control Barrier Function (CBF) technique. Cancer is a complex and highly dynamic disease characterized by uncontrolled cell growth and proliferation. By formulating the cancer dynamics as a control system, this study introduces a CBF-based controller that guides the cancerous tissue towards safe and controlled behaviors. The controller is designed to simultaneously optimize treatment efficacy and patient safety. The methodology involves modeling the cancer growth dynamics, incorporating relevant biological constraints, and designing the CBF-based controller to regulate the tumor's evolution within acceptable bounds. Simulation results demonstrate the effectiveness of the CBF-based strategy in achieving safe and optimal cancer control. The controller showcases the ability to drive the cancerous tissue towards desired states while respecting predefined safety constraints.

1. Introduction

Cancer emerges from cells escaping standard control mechanisms, which can exist due to various causes. Growing cancer statistics are a sign that more emphasis should be placed on improving the efficiency of treatments [1]. The collaboration of medicine and engineering can lead to remarkable progress by scheduling new drug administration, which began years ago. Conventional cancer treatments such as surgery, chemotherapy, and radiotherapy are essential to help patients in the fight against cancer. Despite their significance, it is evident that in some cases, these treatments are not as effective as they need to be [2]. As such, there is a need for alternative therapies that can be used to improve clinical outcomes for patients. As a matter of fact, immunotherapies have become increasingly popular among conventional treatments as anti-tumor activity has improved in recent years [3,4]. This therapy boosts the immune system with external adjuvants, and the body's inherent mechanism aids in cancer treatment by focusing on the immune system rather than the tumor cells [5,6]. It should be noted that eliminating the harmful agents induces toxicity effects on healthy cells and organs in each treatment which requires further studies [7].

The complicated interaction of cells and agents can be described by the mathematical model that facilitates scheduling external drugs as the control input wherein the mathematical model serves as a useful link between the phenomena and the application of control theories. One of the primary goals of a cancer control study is to eliminate tumor cells while reducing the concentration of non-related drug therapy. In [8], the optimal control problem was stated using simple assumptions to minimize tumor size at the end of the treatment period and to keep the normal cell population at an appropriate level as a target to reduce side effects. A problem of optimal control can be solved numerically to achieve objectives, such as control parameterization, which generates a series of approximations and is solved by non-linear programming [9].

Some strategies of control like linear control, bang–bang, quadratic control, and solution of state constraint were comprised for the optimization problem in [10]. A series of estimates of the linear time-variant for the non-linear model has led to the development of a linear quadratic regulator in [11]. A moving horizon estimation-based model predictive control (MPC) has been created by [12], and [13] has shown a proportional–integral–derivative (PID) utilized as an optimal control method. Studies on various control techniques, including a controller based on reinforcement learning with reward functions [14], the application of robust control [15], and a controller employing adaptive-fuzzy theories [16], have been explored in different studies recently.

When administering treatment for a disease, it is essential to acknowledge that side effects may arise independent of individual patient characteristics. Current treatment strategies often neglect to consider potential drug toxicity, highlighting the urgency to account for these side effects, constraints, and control objectives to ensure a safe and effective treatment plan. Depending on the patient's health condition, one of the primary goals of immunotherapy should be to minimize

* Corresponding author at: Process Control Laboratory, Faculty of Natural Sciences and Engineering, Åbo Akademi University, Turku, Finland.
E-mail addresses: z.ahmadi@mehr.pgu.ac.ir (Z. Ahmadi), razminia@pgu.ac.ir, abolhassan.razminia@abo.fi (A. Razminia).

https://doi.org/10.1016/j.mbs.2024.109142
Received 28 August 2023; Received in revised form 12 December 2023; Accepted 9 January 2024
Available online 11 January 2024

toxicity within the body, despite the fact that this may present a technical challenge. In order to address this issue and provide a safe and effective treatment, it is crucial to identify a set of responses that are deemed safe and reliable. Considering such issues in a rigorous mathematical framework, required some advanced theoretical studies which roots in the invariant set theory. As one of the first steps, in the 1940's, a research has been conducted establishing the necessary and sufficient conditions for an invariant set [17]. Subsequently, in the 2000's, barrier certificates were introduced as a method of optimization aimed at ensuring the safety of non-linear and hybrid systems [18–20].

Barrier certificates are a class of continuous functions essential in performance indices. Their primary purpose is to prevent the occurrence of undesirable zones, thus enhancing the safety of complex systems. This approach has been widely adopted in various engineering and related domains, owing to its effectiveness in ensuring safety [21–24]. Furthermore, following the Lyapunov function definition, a continuously differentiable Lyapunov function adheres to inequality conditions and yields level sets. Consequently, this definition has led to the introduction of a "Lyapunov-like" function as a safety barrier function, which causes its values to approach infinity when the states approach the boundary of a set [25]. The barrier function has helped validate the invariant set but has limited use in controller design.

The motivation for accessing control input can be influenced by the Lyapunov function, which was extended to control Lyapunov function (CLF). The CLF is an inspiration for the Control Barrier Function (CBF), which utilizes the barrier function as a safety means. On the other hand, the CBF is a safety control method that ensures that the system stays within a safe set by utilizing a barrier function. System control can be created by combining the CLF with the CBF, stabilizing the system, and ensuring its safety with quadratic programming (QP). It is worth noting that, to the best of our knowledge, while this approach has been effective in developing robots and motion-control systems, its potential applications in the field of cancer have yet to be explored. Some applications of such technique have been studied on the epidemic of Covid-19 by a constraint on the infected population [26,27]. In order to address intricate issues that involve various constraints, implementing a high-order control barrier function (HOCBF) was proposed in [23,24].

Our main contributions can be pursued in the following objectives: incorporating the dynamic characteristics of toxicity levels into the Kirschner–Panetta immunotherapy model; achieving continuous drug administration with optimal control to minimize time and drug consumption using PMP as the reference control with the fewest constraints; implementing CLF as stability constraints to minimize tumor volume while effector cell volume is maintained at the desired value; and investigating safety therapy by constraining toxicity levels in two ways. This achievement has the potential to establish a fundamental basis for the development of innovative clinical trials.

This study provides a detailed discussion of the model in Section 2, followed by a comprehensive explanation of the preliminary in Section 3 and formulation problem in Section 4. The results will be presented through a series of case studies in Section 5. The final section will be concluded and suggest potential research topics for future exploration.

2. Model description

This research employs the Kirschner–Panetta model [2], a widely utilized mathematical model in immunotherapy, to illustrate the central concept of safe-optimal treatment. The mathematical aspects concerning immunotherapy encompass the interplay among effector cells, tumor cells, and cytokine IL_2 concentration through nonlinear terms. The effector cells are assumed to be all activated cells in the immune system that kill tumor cells, while the tumor cells are proliferated cells caused by disease agents. The cytokine IL_2 is a protein that helps plays a role in regulating and distinguishing immune cells. The state-space representation of the model that is considered in our study can be described as follows:

$$\frac{dE(t)}{dt} = \alpha_a T(t) - d_1 E(t) + \frac{\rho_1 E(t)C(t)}{\alpha_{50_1} + C(t)} + a_1 u_1(t) \tag{1}$$

$$\frac{dT(t)}{dt} = r_1 T(t)\big(1 - bT(t)\big) - \frac{c_1 E(t)T(t)}{\alpha_{50_2} + T(t)} \tag{2}$$

$$\frac{dC(t)}{dt} = \frac{\rho_2 E(t)T(t)}{\alpha_{50_3} + T(t)} - d_U C(t) + a_2 u_2(t) \tag{3}$$

where $E(t)$, $T(t)$, and $C(t)$ denote the volume of effector cells, tumor cells, and concentration of cytokine IL_2 at time t, respectively. The control input labeled $u_1(t)$ refers to adoptive cell transfer [28]. The second input, $u_2(t)$, is used to deliver an IL_2 injection as an adjunct for enhancing the immune system.

As shown in Fig. 1, upon detecting a tumor cell, the immune system initiates a cascade of events resulting in the proliferation of effector cells, which is facilitated by intervening IL_2. This proliferation is represented in Eq. (1) as $\alpha_a T(t)$, in which α_a signifies the antigenicity of the tumor. The increasing number of tumor cells leads to the death of effector cells through an apoptosis process, which is determined by the death rate d_1 in the term $d_1 E(t)$. Another proliferation occurs by representing the Michaelis–Menten form as the term $\frac{\rho_1 E(t)C(t)}{\alpha_{50_1}+C(t)}$, defining growth effector cells due to IL_2. The parameters ρ_1 and α_{50_1} determine the immune response rate and half-saturation constant.

Tumor cells need sufficient resources to grow, represented by the term $r_1 T(t)\big(1 - bT(t)\big)$ in Eq. (2). This term considers the growth rate r_1 and the inverse carrying capacity b to model limited resource access. Next, the effector–tumor interaction is defined by terms $\frac{c_1 E(t)T(t)}{\alpha_{50_2}+T(t)}$, which causes a decrease in tumor cells as a competition. Moreover, the nonlinear term $\frac{\rho_2 E(t)T(t)}{\alpha_{50_3}+T(t)}$ describes an increase in the concentration of IL_2 due to the interaction between the effector cell and tumor cell in Eq. (3). The parameters α_{50_2} and α_{50_3} determine the half-saturation constants. The parameter c_1 introduces the competition rate between effector and tumor cells, and the ρ_2 is immune response rates. The effects of each cell on the other are drawn in Fig. 1 by arrows.

The IL_2 protein has a natural depletion modeled by $d_U C(t)$, and d_U is the depletion rate of cytokine in Eq. (3). The body's innate immune system may become weakened when faced with an increased number of tumor cells. As a result, it is necessary to administer an injection of drugs to enhance the immune cells' ability to fight. The latest terms of Eqs. (1) and (3), $a_1 u_1(t)$ and $a_2 u_2(t)$ represent the injection rate of drugs, where a_1 and a_2 are the treatment factors to enhance the effector cell populations and IL_2 concentration, respectively, as shown in Fig. 1. The model has undergone significant improvement, with a notable enhancement being the addition of a dynamic toxicity level. This enhancement now facilitates the measurement of the impact of drugs on the body, providing a more comprehensive understanding of their effects, as detailed below:

$$\frac{dU_{c_1}(t)}{dt} = -\gamma_1 U_{c_1}(t) + u_1(t) \tag{4}$$

$$\frac{dU_{c_2}(t)}{dt} = -\gamma_2 U_{c_2}(t) + u_2(t) \tag{5}$$

$$\frac{dT_x(t)}{dt} = -\eta_e T_x(t) + \sum_{i=1}^{2} T_{xx_i} U_{c_i}(t). \tag{6}$$

The cumulative effect of all enzymatic reactions between the toxic compounds in the drug and the intracellular components determines drug toxicity levels by these equations. The state variables $T_x(t)$ and $U_{c_i}(t)$ define the toxicity level and concentration of drugs, respectively. The concentration of drugs is determined by the decay of each drug, which occurs at a half-life of γ_i in Eqs. (4)–(5). The drug infusion rate is denoted by $u_i(t)$ in all equations for $i = 1, 2$. The toxicity level is calculated by adding up the concentration of drugs multiplied by the impact coefficient T_{xx_i} and decreasing with respect to the metabolic rate of drugs in the body denoted by η_e in Eq. (6). The purpose of

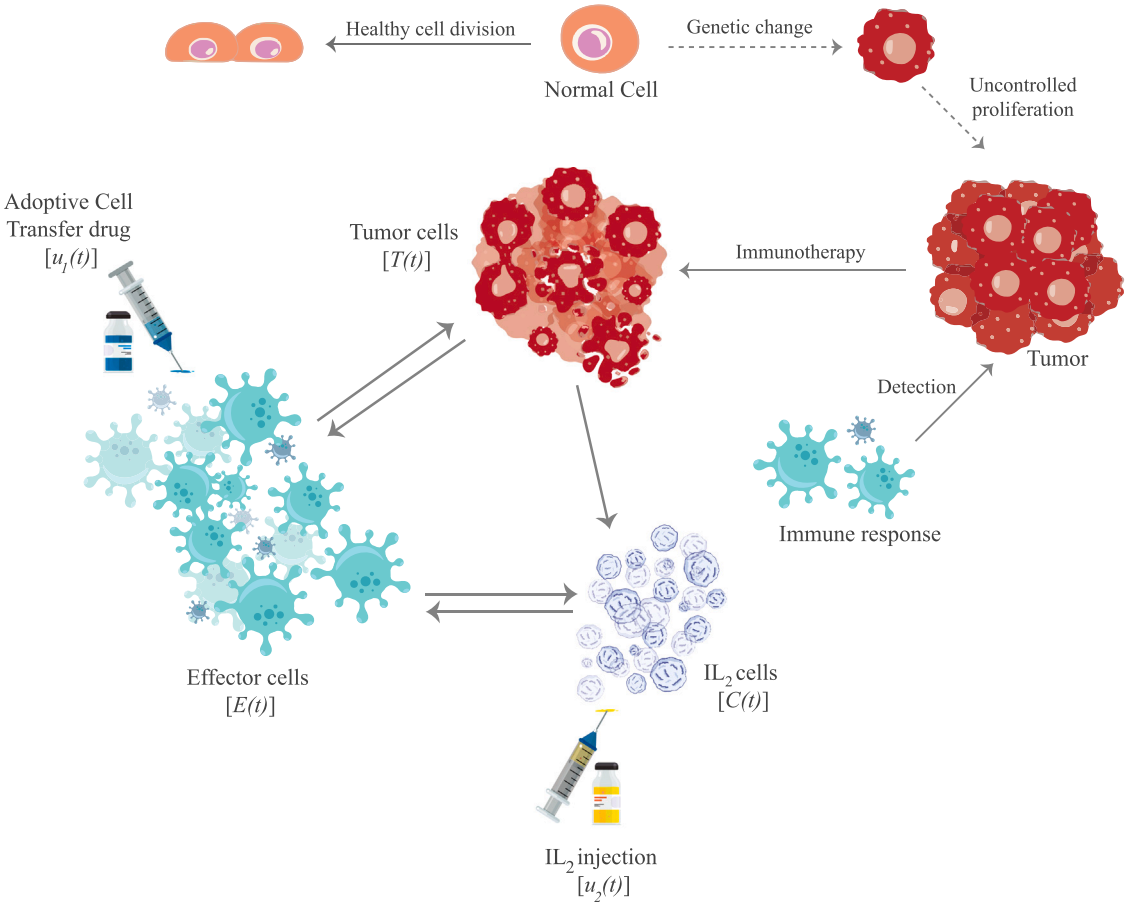

Fig. 1. Tumors develop due to aberrant cell division, which causes the activation of immune system, including immune cells and cytokine IL_2 cells which initiate a cellular assault against the tumor cells via reciprocal interactions. Complicated phases of intercellular interactions have been elucidated by means of the immunotherapy model.

Table 1
Model variable description and unit.

Var.	Description	Unit
$E(t)$	General effector cells	
$T(t)$	Tumor cell	
$C(t)$	Cytokine IL_2 concentration	volume
$U_{c_i}(t)$	Concentration of the drug	
$T_x(t)$	Toxicity level of therapy	
$u_i(t)$	Rate of drug	volume day^{-1}

this study is to examine the stability and safety goals of the combined immunotherapy-toxicity model, which is represented by Eqs. (1)–(6). Tables 1 and 2 provide a brief summary of the variables and parameters used in the model. Lastly, It is worth noting that the medications mentioned in this study have been assessed in a general manner.

3. Preliminaries

The complex cancer dynamic can be elucidated by representing it with a nonlinear vector field denoted as f accompanied by the affine component that encompasses the control parameter u_i in the following manner:

$$\dot{\mathbf{x}} = f(\mathbf{x}) + \sum_{i=1}^{m} g_i(\mathbf{x})u_i \tag{7}$$

in which $\mathbf{x} = [x_1 \quad x_2 \quad \dots \quad x_n]^T \in \mathcal{X} \subset \mathbb{R}^n$ and $\mathbf{u} = [u_1 \quad u_2 \quad \dots \quad u_m]^T \in \mathcal{U} \subset \mathbb{R}^m$ are the state vector and the control input, respectively. The functions $f : \mathbb{R}^n \to \mathbb{R}^n$ and $g = [g_1 \quad g_2 \quad \dots \quad g_m] : \mathbb{R}^n \to \mathbb{R}^{n\times m}$ are assumed globally Lipschitz and g_i is the ith column of the matrix g. The control inputs provide some trajectories according to the objectives or constraints, while trajectories may not always be satisfied to stay in a certain set. However, safety is defined as not exceeding a particular enclosed zone by determining several constraints. To be more exact, in the sequel, formal description of the concepts are given.

A set C is defined as *forward invariant* to an affine system if the unique solution $\mathbf{x}(t)$ stays in the set for every initial state $\mathbf{x}_0 \in C$ in $t \in [t_0, t_{\max})$. In order to describe the movement of the state variable within the forward invariant set, it is beneficial to establish a scalar function, e.g., $h(\mathbf{x})$, that serves as an indicator of the state's condition. A typical representation is as follows:

$$C = \{\mathbf{x} \in D \subset \mathcal{X} : h(\mathbf{x}) \geq 0\} \tag{8}$$

whose boundary, ∂C and interior region, $\mathrm{Int}(C)$, are defined as:

$$\begin{aligned} \partial C &= \{\mathbf{x} \in D \subset \mathcal{X} : h(\mathbf{x}) = 0\} \\ \mathrm{Int}(C) &= \{\mathbf{x} \in D \subset \mathcal{X} : h(\mathbf{x}) > 0\} \end{aligned} \tag{9}$$

which refers to a safe set with a smooth indicator function $h : \mathbb{R}^n \to \mathbb{R}$. According to this definition, a well-known theorem, i.e., the Nagumo theorem, provides a necessary and sufficient condition for a set, C, to be invariant [29]. More specifically, it says that C is invariant if and only if $\dot{h}(\mathbf{x}) \geq 0, \forall \mathbf{x} \in \partial C$. It is clear that the value of the function $h(\mathbf{x})$ is positive within the set and decreases to zero when approaching the boundary. The condition on $\dot{h}(\mathbf{x})$ declares that $h(\mathbf{x})$ should be increased again and pushed back into the set as the boundary and resulting in the verification of Nagumo theorem. Therefore, $h(\cdot)$ can be identified as a barrier function, and its behavior in this set is illustrated in Fig. 2. It is a natural tool to represent and constrain the feasible region of a problem.

Table 2
Description and unit of model parameters.

Param.	Description	Unit	Param.	Description	Unit
α_a	Antigenicity of tumor		b	Reciprocal carrying capacity	unit of volume
ρ_i	Immune response rate		α_{50_i}	Half saturation constant	
d_U	Elimination rate of therapeutic agent	day^{-1}	η_e	Metabolic rate	
d_1	Death rate		γ_i	Half-life depletion rate of drag	day^{-1}
r_1	Growth rate		T_{xx_i}	Toxicity rate of drug	
c_1	Competition rate		a_i	Fractional cell-kill rate due to therapy	–

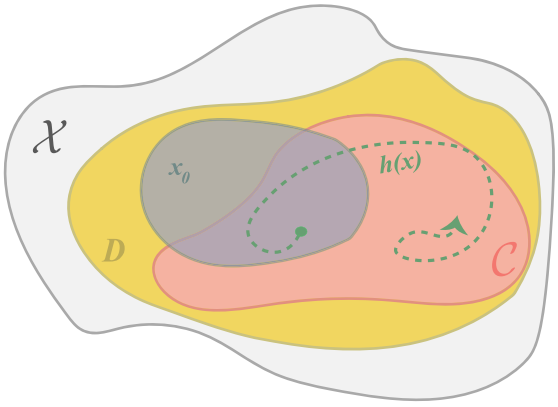

Fig. 2. Typical trajectory of the barrier function in the safe set.

The barrier functions are used in two notions: reciprocal barrier function (RBF) and zeroing barrier function (ZBF), with RBF's seen as logarithmic or inverse forms of ZBF's as

$$B(\mathbf{x}) = -\log\left(\frac{h(\mathbf{x})}{1+h(\mathbf{x})}\right) \quad \text{or} \quad B(\mathbf{x}) = \frac{1}{h(\mathbf{x})} \tag{10}$$

while this function should satisfy the properties

$$\inf_{\mathbf{x}\in \mathrm{Int}(C)} B(\mathbf{x}) \geq 0, \qquad \lim_{\mathbf{x}\to\partial C} B(\mathbf{x}) = \infty. \tag{11}$$

According to definition (9), the barrier function $h(\cdot)$ is a ZBF equaled to zero when the trajectory hits the set's boundary, resulting in the RBF being set to infinity at that point. The infinity values of the RBF give unbounded properties that may be unfavorable for implementation in real-time or embedded systems, making ZBF the recommended option. Therefore, the barrier function will henceforth refer to the ZBF.

The initial principles of theories and system information have been raised to facilitate comprehension of further details. Lastly, the following definitions are presented in sequence.

Def. A scalar continuous function $\alpha : [0, a) \to [0, \infty)$ is defined to belong a class $\mathcal{K}$, for $a > 0$ if it is strictly increasing and $\alpha(0) = 0$.

Def. A continuous function $\alpha : [-b, c) \to [-\infty, \infty)$ is called an *extended class* $\mathcal{K}$, for $b, c > 0$, denoted by $\mathcal{K}_e$, if it is strictly increasing and $\alpha(0) = 0$.

4. Main method

The barrier function takes inspiration from the Lyapunov function. The Lyapunov function can evaluate the convergence to a specific point (like an equilibrium point) without the need for computing the exact solution. The control Lyapunov function (CLF) has been defined, corresponding to stabilizing and controlling a system. It is specified for the positive function $V(\mathbf{x}) : \mathbb{R}^n \to \mathbb{R}^{\geq 0}$ as

$$\dot{V}(\mathbf{x}, \mathbf{u}) = L_f V(\mathbf{x}) + \sum_{i=1}^{m} L_{g_i} V(\mathbf{x}) u_i \leq -\lambda\big(V(\mathbf{x})\big), \tag{12}$$

where the derivative function $\dot{V}(\mathbf{x}, \mathbf{u})$ is the negative function that descends by the rate of the class $\mathcal{K}$ function $\lambda(\cdot)$. The Lie derivative $L_{X(\cdot)}Y(\cdot) = \langle \nabla Y(\cdot), X(\cdot)\rangle$ is used for indicating the derivative of $V(\mathbf{x})$ with respect to $f(\mathbf{x})$ and $g_i(\mathbf{x})$ with specifying $L_f V(\mathbf{x})$ and $L_{g_i} V(\mathbf{x})$ respectively. Thus, stability objectives can be defined by inequality constraints that make the function $V(\mathbf{x})$. These objectives are often considered for minimizing the number of tumor cells while maintaining the number of effector cells for modeling cancer systems. Stability is finally reached by determining the control input to satisfy the condition (12). The set of CLF inputs is considered as,

$$K_{clf}(\mathbf{x}) = \{u \in \mathcal{U} : L_f V(\mathbf{x}) + \sum_{i=1}^{m} L_{g_i} V(\mathbf{x}) u_i + \lambda\big(V(\mathbf{x})\big) \leq 0\}. \tag{13}$$

Ensuring safety is a critical component of any system, and it requires control input that satisfies the safety constraint. Unlike stability, safety must be maintained for the duration of any trajectory rather than just at the final point. Therefore, the function $h(\cdot)$ is defined for the forward invariant set C by the CLF motivation, with the safety constraint declared as satisfying definition (8)–(9). The barrier function cannot be directly used for system control. Therefore, the control barrier function is defined as follows:

Def. Consider the affine system (7) and the set C defined by (8)–(9), the continuously differentiable function $h(\cdot) : \mathrm{R}^n \to \mathrm{R}$ is called a control barrier function if there exists an extended class $\mathcal{K}$ function $\alpha(\cdot)$ for all $\mathbf{x} \in \mathbf{D}$ with $C \subseteq D \subset \mathrm{R}^n$ such that

$$\sup_{\mathbf{u}\in U}\Big(L_f h(\mathbf{x}) + \sum_{i=1}^{m} L_{g_i} h(\mathbf{x}) u_i + \alpha(h(\mathbf{x}))\Big) \geq 0.$$

The objective behind the enactment of $\alpha(h(\mathbf{x}))$ is to mitigate the tendency of conservation of responses, thereby facilitating the development of more fitting controllers for heuristically determined practical implementations. Furthermore, by incorporating this term, it becomes easier to compare it to CLF. Thus, the set of controllers is described by this definition CBF a

$$K_{cbf}(\mathbf{x}) := \{\mathbf{u} \in \mathcal{U} : L_f h(\mathbf{x}) + \sum_{i=1}^{m} L_{g_i} h(\mathbf{x}) u_i + \alpha(h(\mathbf{x})) \geq 0\}. \tag{14}$$

Once more, if $\alpha(\cdot)$ and $\dot{h}(\cdot)$ are both locally Lipschitz continuous, then the CBF is locally Lipschitz continuous.

Separate CLFs and CBFs can be used to establish the objectives and constraints of a system. These inequality constraints, identified as (13) and (14), are affine and linear to the control input. As a result, they can be combined to determine the appropriate control input that satisfies the constraints. This unification process can be achieved by employing quadratic programming (QP) as

$$\begin{aligned}(\mathbf{u}(t), \delta) = \quad & \underset{(\mathbf{u},\delta)\in\mathbb{R}^{m+1}}{\arg\min} \quad \Big(\|\mathbf{u}(t) - \mathbf{u}_{ref}(t)\|^2 + p\delta^2\Big) \\ & s.t. \quad L_f V(\mathbf{x}) + \textstyle\sum_{i=1}^{m} L_{g_i} V(\mathbf{x}) u_i \leq -\lambda\big(V(\mathbf{x})\big) + \delta \\ & \qquad L_f h(\mathbf{x}) + \textstyle\sum_{i=1}^{m} L_{g_i} h(\mathbf{x}) u_i \geq -\alpha(h(\mathbf{x})),\end{aligned} \tag{15}$$

which its convexity form is suitable for real-time application. The control input $\mathbf{u}(t)$ obtained from the QP aims to achieve stability and safety by balancing between them. Although there are multiple constraints, they must be prioritized during implementation. Therefore, safety is the top priority and is treated as a hard constraint. Meanwhile, stability is a soft constraint, and the variable δ is defined as the relaxation, weighted by the penalizing coefficient p in the QP. The QP formulation allows for incorporating a reference input, $\mathbf{u}_{ref}(t)$, which

Table 3
Parameters of the model.

Para.	Value	Para.	Value	Para.	Value
α_a	0–0.05	ρ_1	0.1245	γ_1	0.27
α_{50_1}	2×10^7	ρ_2	5	γ_2	0.2
α_{50_2}	1×10^5	r_1	0.18	T_{xx_1}	1
α_{50_3}	1×10^3	c_1	1	T_{xx_2}	1
b	1×10^{-9}	d_1	0.03	a_1	500
η_e	0.4	d_U	10	a_2	7×10^7

may entail any control strategy. This study considers it the optimal control by utilizing Pontryagin's minimum principle for minimizing fuel and time. This enables the QP to effectively integrate various objectives straightforwardly without the need for complex solving. As a result, the solution provided delivers a sub-optimal response.

Sometimes, the conditions in the QP may be modified to identify a more comprehensive safe set or to resolve the problem under multiple conditions. One of these is particularly relevant when dealing with safety constraints for nonlinear systems. A practical approach to implementation involves selecting the control barrier function by a relative degree greater than one, which is defined as the function $h(\mathbf{x})$ with the relative degree r as

$$h^{(r)}(\mathbf{x},\mathbf{u}) = L_f^{(r)}h(\mathbf{x}) + \sum_{i=1}^{m} L_{g_i}L_f^{(r-1)}h(\mathbf{x})u_i$$

that $L_{g_i}L_f^{(r-1)}h(\mathbf{x}) \neq 0$ and $L_{g_i}L_f^{(j)}h(\mathbf{x}) = 0$, $j \in \{1,\dots,r-2\}$ for all $\mathbf{x} \in D$. Therefore, the inequality condition to subject the QP must be changed to a linear and affine condition for $\mathbf{u}(t)$. Although a definitive method for solving this challenge has not yet been found, one potential solution involves using the sequence of the function $\boldsymbol{\Phi}_j(\mathbf{x})$ as:

$$\begin{aligned}&\boldsymbol{\Phi}_0(\mathbf{x}) = h(\mathbf{x})\\ &\boldsymbol{\Phi}_j(\mathbf{x}) = \dot{\boldsymbol{\Phi}}_{j-1}(\mathbf{x}) + \varphi_j(\boldsymbol{\Phi}_{j-1}(\mathbf{x})), \quad j \in \{1,\dots,r\},\end{aligned} \tag{16}$$

where $\varphi_j(\cdot)$ is a $(r-j)$th order differentiable class $\mathcal{K}$ function. A sequence of corresponding super-level sets follows as

$$C_j = \{\mathbf{x} \in D : \boldsymbol{\Phi}_j \geq 0\}, \quad j \in \{1,\dots,r\}. \tag{17}$$

It is well-known that if C_r is forward invariant and $\mathbf{x}_0 \in \bigcap_{j=0}^{r} C_j$, then C is forward invariant [30].

Now, the high-order control barrier function (HOCBF) can be defined as

Def. A function $h(\mathbf{x}) : D \in \mathbb{R}^n \to \mathbb{R}$ is a high-order control barrier function of a relative degree r for an affine system by considering $\boldsymbol{\Phi}_j(\cdot)$ defined in (16) and its associated set C_j (17) for $j \in \{1,\dots,r\}$, if there exist $(r-j)$th order differentiable class $\mathcal{K}$ functions $\varphi_j(\cdot)$, $j \in 1,\dots,r-1$ and a class $\mathcal{K}$ function $\varphi_r(\cdot)$ such that

$$\sup_{\mathbf{u}\in\mathcal{U}}[L_f^r h(\mathbf{x}) + \sum_{i=1}^{m} L_{g_i}L_f^{r-1}h(\mathbf{x})u_i + \alpha(h(\mathbf{x})) + v_r.\varphi_r(\boldsymbol{\Phi}_{r-1}(\mathbf{x}))] \geq 0 \tag{18}$$

for all $\mathbf{x} \in C_1 \bigcap \cdots \bigcap C_r$ and the parameter v_j for $j \in 1,\dots,r$ is included to minimize a conflicting effect among constraints.

So, it is necessary to modify the constraint of the HOCBF in the QP formulation. After that, the new formulation is rewritten to determine proper control inputs in the QP as

$$\begin{aligned}(\mathbf{u}(t),\delta) = \quad & \underset{(\mathbf{u},\delta)\in\mathbb{R}^{m+1}}{\arg\min} \quad \left(\|\mathbf{u}(t)-\mathbf{u}_{ref}(t)\|^2 + p\delta^2\right)\\ & s.t. \quad L_f V(\mathbf{x}) + \textstyle\sum_{i=1}^{m} L_{g_i}V(\mathbf{x})u_i \leq -\lambda\big(V(\mathbf{x})\big) + \delta\\ & \quad L_f^r h(\mathbf{x}) + \textstyle\sum_{i=1}^{m} L_{g_i}L_f^{r-1}h(\mathbf{x})u_i \geq -\alpha(h(\mathbf{x}))\\ & \quad -v_r.\varphi_r(\boldsymbol{\Phi}_{r-1}(\mathbf{x})).\end{aligned} \tag{19}$$

The results of the method will be investigated in the many case studies for enhancing treatment in the following. The stability objectives will be considered to minimize the tumor cells, as demonstrated in previous studies. Furthermore, the safety constraints will be discussed on the concentration of drugs and toxicity level.

The concise and informative pseudocode summary of the control method is provided herein, which serves as a valuable tool for facilitating easy tracking. The summary offers a clear and comprehensive overview of the implementation and control method as

---

Specify $\mathbf{u}_{ref}$
Lyp Func: K_{clf}
if J only satisfies the stability **then**
  Solve QP in Eq. (15) without the safety constraint.
else
  Brr Fun: K_{cbf}
  if $r = 1$ **then**
    Solve QP in Eq. (15)
  else
    Solve QP in Eq. (19)
  end if
end if

---

5. Case studies and results

The control strategies have been studied by focusing on optimizing drug consumption and minimizing tumor volume so far. However, a comprehensive administration for any therapy must contain side effects. So, the present study confirmed the findings about safe controllers by utilizing CBF. This method provides safety for the immunotherapy-toxicity model (1)–(6) in the affine description (7) with $\mathbf{x} = \begin{bmatrix}E(t) & T(t) & C(t) & U_{c_1}(t) & U_{c_2}(t) & T_x(t)\end{bmatrix}$ and $\mathbf{u} = \begin{bmatrix}u_1(t) & u_2(t)\end{bmatrix}^T$ as

$$f(\mathbf{x},t) = \begin{bmatrix} \alpha_a T(t) - d_1 E(t) + \frac{\rho_1 E(t)C(t)}{\alpha_{50_1}+C(t)} \\ r_1 T(t)\big(1-bT(t)\big) - \frac{c_1 E(t)T(t)}{\alpha_{50_2}+T(t)} \\ \frac{\rho_2 E(t)T(t)}{\alpha_{50_3}+T(t)} - d_U C(t) \\ -\gamma_1 U_{c_1}(t) \\ -\gamma_2 U_{c_2}(t) \\ -\eta_e T_x(t)\sum_{i=1}^{2} T_{xx_i}U_{c_i}(t) \end{bmatrix} \quad g = \begin{bmatrix}g_1 & g_2\end{bmatrix} = \begin{bmatrix} a_1 & 0 \\ 0 & 0 \\ 0 & a_2 \\ 1 & 0 \\ 0 & 1 \\ 0 & 0 \end{bmatrix}$$

with the valued parameters in Table 3 by restricting toxicity due to the concentration drug, which is investigated in two ways: the CBF on the concentration drug and the HOCBF on the toxicity. The schematic of this control strategy is shown in Fig. 3; it is supposed to be implemented in three steps. First, the optimal controller is designed to be subject to the affine model by certain constraints under states and control input with given conditions and a specific performance index. Next, defining the objectives for stability and safety by the function of states, and finally, unifying in the QP.

Optimal response

The optimal problem is focused on therapy time and consumption of drugs. Therefore the performance index is defined for the free final time as simply as

$$\min_{\mathbf{x},\mathbf{u},t} \int_{t_0}^{t_f} \|\mathbf{u}(t)\|^2 \mathrm{d}t. \tag{20}$$

The affine model (1)–(6) is subject to this performance index by considering all states' initial values and the final value of tumor value as $A(t_f) = \epsilon$ as point constraints. Additionally, some inequality state-control constraints are specified for obtaining a reasonable response as

$$C(t) \leq 3\times10^4, \text{ and } 0 \leq \mathbf{u}(t) \leq 1.$$

Thus, the first step is structured to obtain reference input $\mathbf{u}_{ref}(t)$ by the requirements of the problem, as shown in Fig. 3. Open-OCL [31] solves the optimal problem due to the complex model numerically.

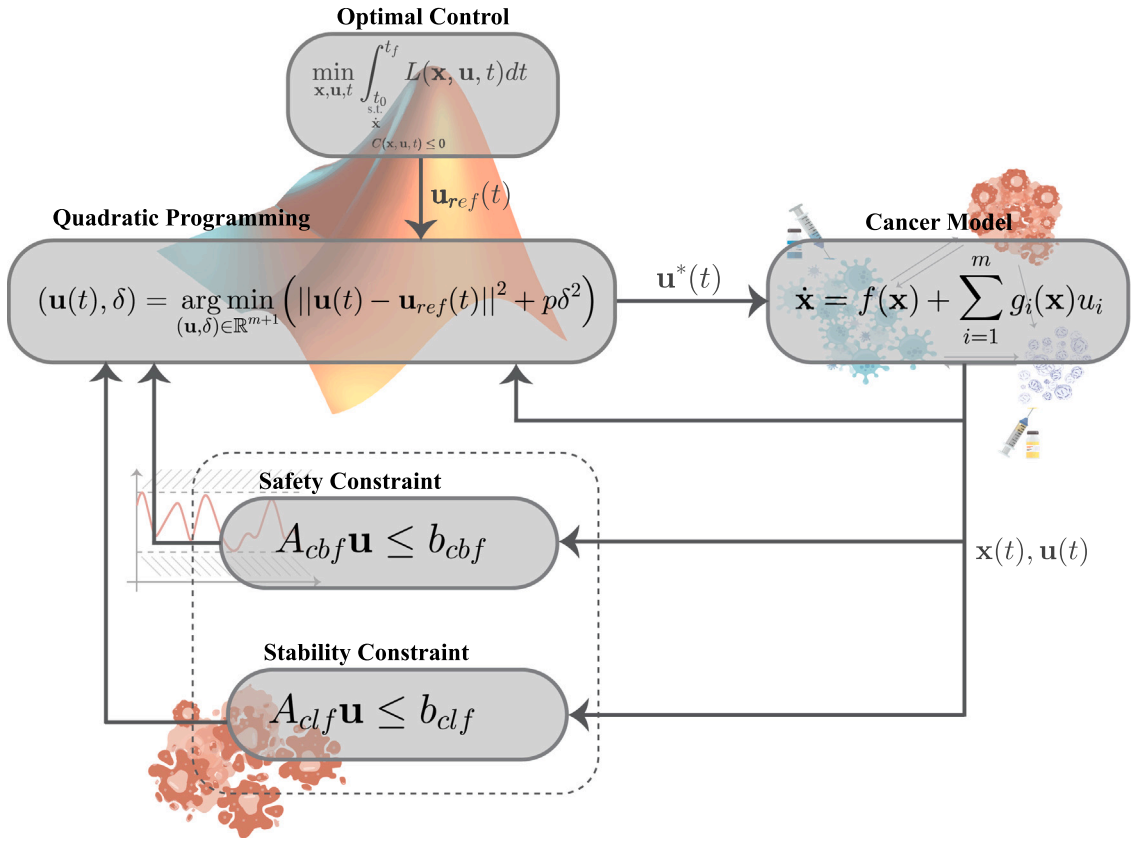

Fig. 3. Schematic of the optimal control barrier function approach.

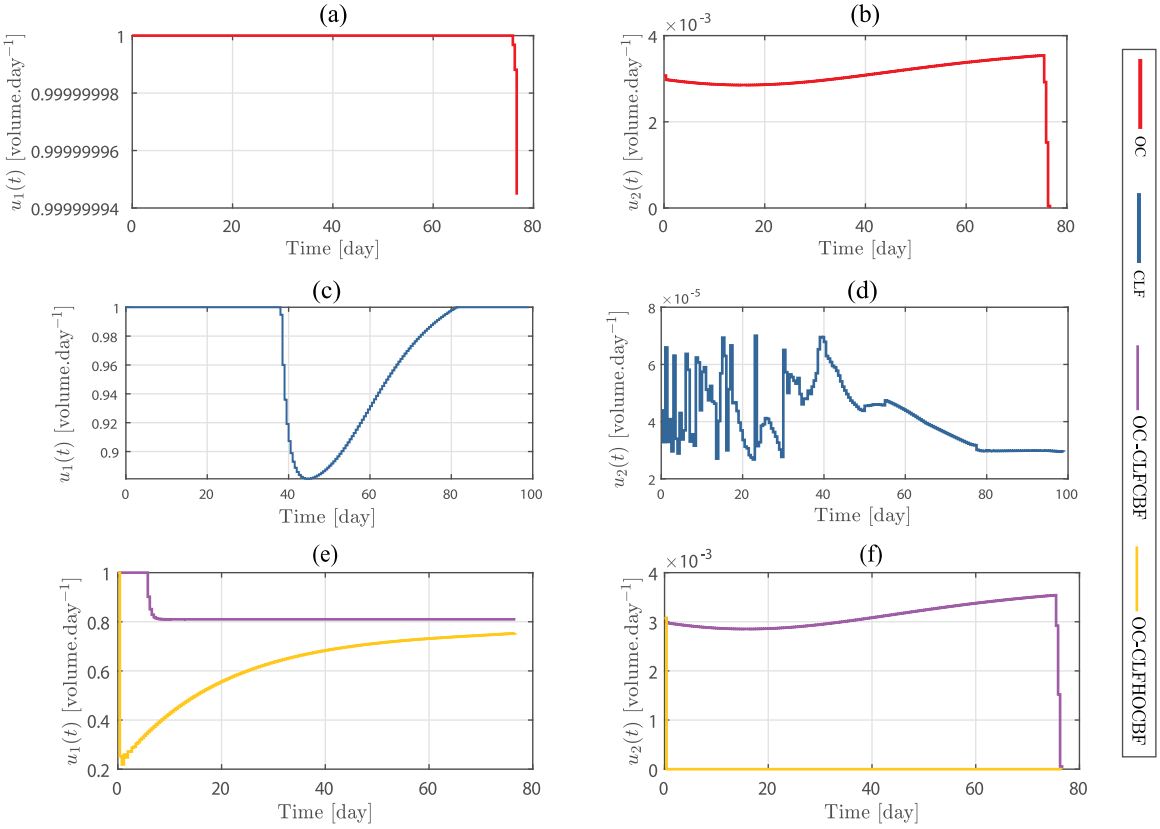

Fig. 4. The rates of drugs administered are illustrated for the first and second infusions in (a, b) as optimal control by satisfying conditions, (c, d) using CLF by choosing parameters $\mu_1 = 10$ and $E_v = 2.2 \times 10^4$, and (e, f) using OC-CBF and OC-HOCBF for implementing stable and safe responses under optimality.

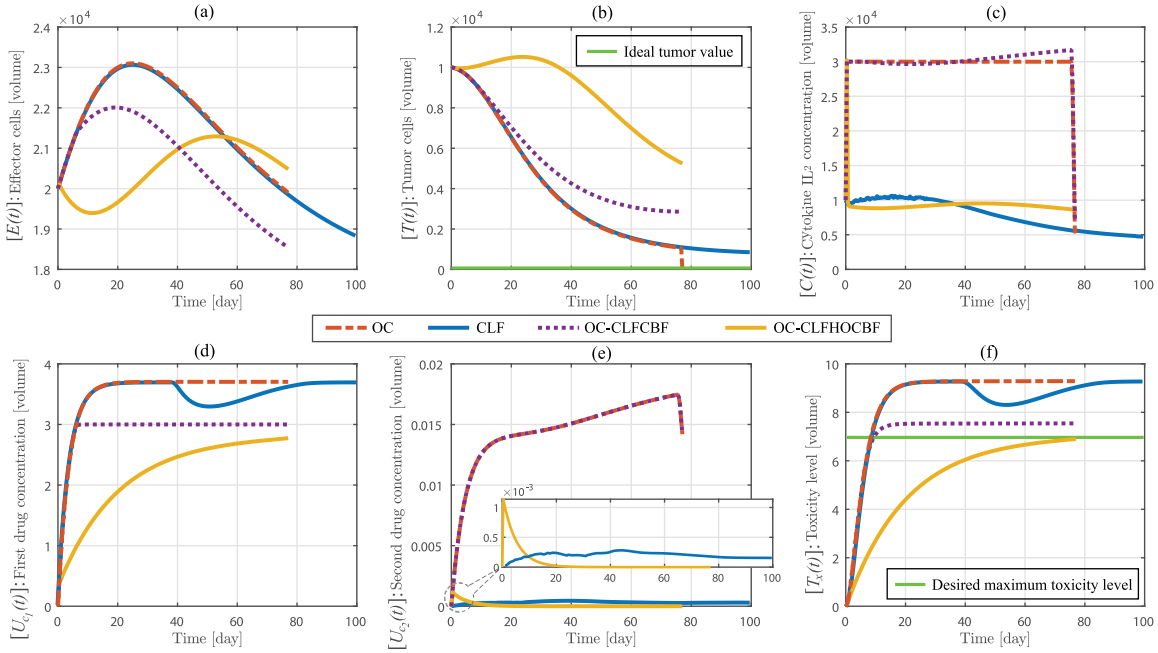

Fig. 5. Changes in states of the immunotherapy-toxicity model for the parameter $\alpha_a = 0.035$ are depicted subject to fuel-time optimal control under point and boundary conditions, control Lyapunov function (CLF) to stability without any reference path, and control barrier functions (CBFs) by constraining drug concentration and toxicity level based on optimal reference response.

Considering the Eqs. (1)–(3), the final point constraint on tumor cells is satisfied by the indirect effect of both control inputs. So, they must be consumed to minimize the index while maintaining the point and boundary constraints. The coefficient of rate first drug is significantly less than the second drug, according to Table 3; hence, the second drug is consumed at the low range, as shown in parts (a) and (b) of Fig. 4. However, to optimize time, they select maximum values that allow the boundary condition. After that concentration of IL_2 increases until the allowed boundary and causes no decrease in the volume of effector cells when there is a large volume of tumor cells. Assuming $\epsilon = 0$, it occurs in less than 80 days. The results have demonstrated the trajectory of states in Fig. 5. Therefore, the values of cells are compelling, and the concentration drug and toxicity values are acceptable as long as no condition is included in them and will be further discussed and compared.

Stability investigation

The level of stability of a system is crucial in determining its effectiveness. In the case of the cancer model, the aim is to reduce the number of tumor cells that can be realized using CLF. The easiest way to select the positive function for this method is to choose a quadratic term of tumor cells. However, Eq. (2) reveals that a function solely incorporating the tumor cell state variable would not achieve stability, as there is no presence of control inputs in its derivative. As a result, it is more fitting to utilize effector cell terms to attain the desired value. The candidate function is selected as

$$V(\mathbf{x}) = \mu_1 T(t)^2 + T(t)(E_v - E(t)) + (E_v - E(t))^2$$

where E_v serves as the desired parameter for the effector cells to achieve as the tumor cells decrease to a minimum value by minimizing the difference between them. The resulting binomial expansion is positive, and the set of stable controllers is determined by employing CLF by Eq. (13).

The stabilization outcomes were achieved by applying QP in (15), without reference input or related constraints, over a specific time horizon. Investigating this result enables one to perceive the potential of the CLF response alone, and it could prove useful in distinguishing variations in subsequent results. It is important to note that the value assigned to the particular function and parameter, λ and p, respectively, can considerably impact the resulting outcomes. In the study of function class $\mathcal{K}$, it is deemed $\lambda(V(\mathbf{x})) = \lambda V(\mathbf{x})$, and a suitable coefficient λ must be chosen. It is important to note that choosing a small value for both λ and p simultaneously may fail to achieve stability objectives. Conversely, selecting significant values for both parameters may lead to non-smooth control input. Therefore, a trade-off between the two is necessary, where a large value for one parameter requires a small value for the other. It is important to consider that selecting a small value of p results in an actively relaxed CLF in the QP, which may not be suitable when dealing with several constraints. In light of this, it is recommended to choose a small value for λ and a large value for p.

The control input outcomes are depicted by selecting $\lambda = 1$ and $p = 200$ in parts (c) and (d) of Fig. 4. The value of $u_1(t)$ changes smoothly, and $u_2(t)$ takes small values, and the changes are reasonable due to the time scale being a day. It should be noted that these outcomes are situated in a lower range than optimal drug use results. These control input outcomes bring about the growth of cells shown in parts (a–c) of Fig. 5. The changes of the effector cells and tumor cells are similar to optimal responses until optimal time; however, the values of tumor cells do not reach zero but have a small final volume. The IL_2 concentration does not increase following the infusion rate $u_2(t)$ compared to optimal response. Consequently, the rate $u_2(t)$ manifests the effect of changing in limited ranges on the state variable $U_{c_2}(t)$. The decreasing growth of $u_1(t)$ on day 40 to about 50 also shows its effect in $U_{c_1}(t)$. Considering that the concentration values of the first drug are higher than the second drug, the effect of this decreasing growth on toxicity is also evident, as seen in parts (d–f) of Fig. 5.

Optimality/safety investigation

So far, the study has found the optimal and stable response, but the primary purpose of this study is to explore the safe response. As previously mentioned, this study is dedicated to prioritizing the safety of this model (1)–(6) by conducting a thorough analysis of its toxicity levels. Our approach to addressing this matter involves an examination from two standpoints. The level of toxicity is directly related to the

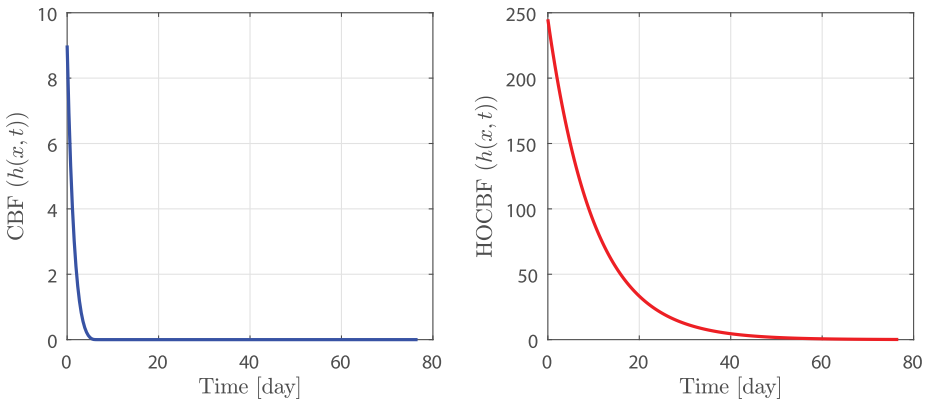

Fig. 6. The results are provided in CBF by choosing $U_{c_{1_{\max}}} = 3$ and $\alpha_1 = 0.66$ and HOCBF by choosing $T_{x_{\max}} = 7$, $\nu_1 = 5$, $\nu_2 = 0.01$, and with the extended class $\mathcal{K}$ as $\alpha(.) = 0.1h(\mathbf{x})$.

concentration of drugs, with the first concentration having a more significant impact due to its higher volume consumption. Thus, the concentration of the first drug is limited in the first standpoint. Assuming that the value of $U_{c_1}(t)$ must not exceed $U_{c_{1_{\max}}}$, then the CBF is selected as follows,

$$h(\mathbf{x}) = \left(U_{c_{1_{\max}}} - U_{c_1}(t)\right)^2 \geq 0.$$

The control safe set is obtained by selecting the proper extended class $\mathcal{K}$, which is considered as $\alpha(.) = \alpha_1 h(\mathbf{x})$ in this case by Eq. (14). In order to effectively enforce hard constraints during unification, it is crucial to select the appropriate parameter carefully. Given the presence of stability and safety constraints, it is advised that this parameter be even stricter than the parameter λ, which can be achieved using a smaller value. The second standpoint entails a direct consideration of toxicity constraints. By selecting the maximum value $T_{x_{\max}}$, the simple function $h(\mathbf{x})$ is chosen as follows,

$$h(\mathbf{x}) = \left(T_x(t) - T_{x_{\max}}\right)^2 \geq 0.$$

After analyzing this function, it has become evident that no discernible control input is present. However, upon further examination of the second derivative, it is apparent that control input is present, indicating that the function has a relative degree of two. So according to the HOCBF definition and the sequence function $\varphi_i(\cdot)$, Eq. (18) is determined as

$$\sup_{\mathbf{u}\in\mathcal{U}} [L_f^2 h(\mathbf{x}) + L_g L_f h(\mathbf{x})\mathbf{u} + \nu_1 \left(T_x(t) - T_{x_{\max}}\right)^2 + \nu_2 T_x(t)] \geq 0.$$

In the preceding stages, the reference control input and stability constraints were precisely delineated, and each CBF and HOCBF function has been specified at this point. Therefore, the requirements for achieving a safe and optimal response are provided in which the QP unifies the constraints by using the formulations (15) and (19) for CBF and HOCBF, respectively. The outcomes of this unification are acquired according to the optimal time horizontal, where $t_f < 80$ illustrates the unified process's efficacy in attaining optimal results within a designated time, as illustrated in the Figs. 5, 4, and 6. Upon examination of the CBF control inputs in Fig. 4, it is evident that the lack of limitations on the second input leads to an infusion rate that closely resembles the optimal response. This is manifested in the alterations observed in the concentration of IL_2 and the second drug, which are influenced by the second input, see parts (c) and (e) in Fig. 5.

In the beginning, the first control input is set to the highest possible value until the concentration of the first drug reaches its peak; then, the input value decreases, as shown in part (d) of Fig. 5 and parts (e) and (f) of Fig. 4. Once the drug concentration reaches its maximum value, the CBF value drops to zero and remains at zero as long as it stays at the safe set, as depicted in Fig. 6. Due to the reduction and strictness of this constraint, the number of tumor cells has decreased below the optimal level. However, the final count is around a third of the initial, which is acceptable. Additionally, the number of effector cells is still within the appropriate range. See parts (a) and (b) of Fig. 5.

It is clear that the toxicity level can be restricted by binding the drug concentration. Alternatively, a specific constraint can be set on the toxicity level directly. However, selecting the appropriate function $h(\mathbf{x})$ becomes more complex when the relative degree is greater than one. The results are also displayed in the figures with the proper parameter selection to obtain a set of appropriate responses. The condition has practical implications that affect both control inputs. As illustrated in parts (e) and (f) of Fig. 4, the infusion rate of the second drug remains almost zero, except for the initial days. The first drug shows exponential growth with lower amounts than in other cases.

These control inputs effectively enforce the safety condition. As the state $T_x(\mathbf{x})$ approaches its maximum threshold value $T_{x_{\max}}$, the control function $h(\mathbf{x})$ progressively diminishes towards zero, depicted in Fig. 6. Based on the state variable changes depicted in Fig. 5, the current administration has resulted in the tumor cell volume with only half the initial value remaining. However, there has been an increase in the number of effector cells, which now exceeds the initial value. After considering both variables, the result can be considered satisfactory.

6. Conclusion and discussion

In this study, the safe treatment was addressed in the model by implementing the control barrier function method. The examined model is a combination of the Kirschner–Panetta immunotherapy model and the dynamics of drug toxicity, including drug concentration and level of toxicity. This combination has the potential to quantify and restrict the toxicity of medications in order to guarantee safer treatment. Drug concentration is comprised of the drug rate, a control input, and the rate at which the concentration decays. Toxicity level is also determined through the summation of drug concentrations, their corresponding impact coefficients, and a degradation term associated with toxicity. The Kirschner–Panetta model for association toxicity has been established as an adequate foundation for investigation.

Achievement of the final response by using this method was considered in three steps. First, the optimal control was obtained by specifying the simple performance index and constraints using PMP, which provided the reference input for the following steps. Next, the CLF was used to provide stability concurrently with safety in administration, which was brought about by reducing the volume of tumor cells. On the other hand, according to the formulation of it, which is linear and affine concerning the control input, it is possible to unify different constraints of stability and safety by using QP.

The examination of safety was approached from two standpoints: Firstly, the constraint placed on the concentration of drugs, and secondly, the constraint placed on the level of toxicity. Based on the system dynamic, it can be inferred that the toxicity level is also limited when

the drug concentration is kept within limits. Safety is achieved through CBF with a relative degree of one. Choosing an appropriate function with a relative degree of one makes it easier to obtain a suitable set of responses with less difficulty. The next point was to directly limit the toxicity level, which leads to choosing a function with a relative degree greater than one, also known as HOCBF. However, this can make selecting the proper function more difficult and result in a more conservative response.

The current study utilized a widely accepted model in the field, but it may not accurately represent the study population or medications being investigated. Therefore, the integration of clinical data holds promise for furnishing a more nuanced and dependable response in subsequent research endeavors. In this regard, it should be mentioned that the model has been evaluated based on precise parameters and measurable variables. So, future research could benefit from investigating models with uncertainty using a robust control barrier function strategy and observable filters such as the Kalman filter.

Modifying the boundary on variables or coefficients of controllers under a particular drug can also add greater realism. Prospective investigations are encouraged to direct attention towards the formulation of algorithms for the most suitable HOCBF (or CBF), thereby diversifying the array of available options. The continuous-time approach for obtaining drug rate results in each step is recommended over previous studies that relied on piecewise assumptions, as it increases efficiency. However, implementing this approach in real-world scenarios requires prerequisite medical equipment. Despite this, it presents an opportunity to advance the field.

CRediT authorship contribution statement

Zahra Ahmadi: Formal analysis, Methodology, Visualization, Writing – original draft. **Abolhassan Razminia:** Conceptualization, Formal analysis, Methodology, Project administration, Supervision, Validation, Visualization, Writing – original draft, Writing – review & editing.

Declaration of competing interest

The authors declared no potential conflicts of interest with respect to the research, authorship, and/or publication of this article.

Funding acknowledgment

The authors received no financial support for the research, authorship, and/or publication of this article.

References

[1] R. Khademi, A. Razminia, Selective nano-thermal therapy of retinoblastoma in human eye during retinal laser surgery (vol 24 pg 102102, 2020), Nanomed.-Nanotechnol. Biol. Med. 40 (2022).
[2] D. Kirschner, J.C. Panetta, Modeling immunotherapy of the tumor–immune interaction, J. Math. Biol. 37 (1998) 235–252.
[3] S.A. Rosenberg, Entering the mainstream of cancer treatment, Nat. Rev. Clin. Oncol. 11 (11) (2014) 630–632.
[4] K. Ellis, C.A. Pennell, Demystifying cancer immunotherapy for lay audiences, Front. Immunol. 10 (2019) 2488.
[5] F.D. Barber, Recent developments in oncology immunotherapy, adverse effects part 2, J. Nurse Pract. 14 (4) (2018) 259–266.
[6] J. Couzin-Frankel, Cancer immunotherapy, 2013.
[7] H. Schättler, U. Ledzewicz, Optimal control for mathematical models of cancer therapies, in: An Application of Geometric Methods, Springer, 2015.
[8] J. Murray, Optimal control for a cancer chemotheraphy problem with general growth and loss functions, Math. Biosci. 98 (2) (1990) 273–287.
[9] R.B. Martin, Optimal control drug scheduling of cancer chemotherapy, Automatica 28 (6) (1992) 1113–1123.
[10] L.G. de Pillis, W. Gu, K.R. Fister, T. Head, K. Maples, A. Murugan, T. Neal, K. Yoshida, Chemotherapy for tumors: An analysis of the dynamics and a study of quadratic and linear optimal controls, Math. Biosci. 209 (1) (2007) 292–315.
[11] M. Itik, M.U. Salamci, S.P. Banks, Optimal control of drug therapy in cancer treatment, Nonlinear Anal. TMA 71 (12) (2009) e1473–e1486.
[12] T. Chen, N.F. Kirkby, R. Jena, Optimal dosing of cancer chemotherapy using model predictive control and moving horizon state/parameter estimation, Comput. Methods Programs Biomed. 108 (3) (2012) 973–983.
[13] B.G. Czakó, J. Sápi, L. Kovács, Optimal PID based computed torque control of tumor growth models, IFAC-PapersOnLine 51 (4) (2018) 900–905.
[14] R. Padmanabhan, N. Meskin, W.M. Haddad, Reinforcement learning-based control of drug dosing with applications to anesthesia and cancer therapy, in: Control Applications for Biomedical Engineering Systems, Elsevier, 2020, pp. 251–297.
[15] K. Moussa, M. Fiacchini, M. Alamir, Robust optimal scheduling of combined chemo-and immunotherapy: Considerations on chemotherapy detrimental effects, in: 2020 American Control Conference, ACC, IEEE, 2020, pp. 4252–4257.
[16] M. Sarhaddi, M. Yaghoobi, A new approach in cancer treatment regimen using adaptive fuzzy back-stepping sliding mode control and tumor-immunity fractional order model, Biocybern. Biomed. Eng. 40 (4) (2020) 1654–1665.
[17] M. Nagumo, Über die lage der integralkurven gewöhnlicher differentialgleichungen, Proc. Phys.-Math. Soc. Jpn. 3rd Ser. 24 (1942) 551–559.
[18] S. Prajna, A. Jadbabaie, Safety verification of hybrid systems using barrier certificates, in: HSCC, vol. 2993, Springer, 2004, pp. 477–492.
[19] S. Prajna, Barrier certificates for nonlinear model validation, Automatica 42 (1) (2006) 117–126.
[20] J. Nocedal, S.J. Wright, Quadratic programming, in: Numerical Optimization, Springer, 2006, pp. 448–492.
[21] P. Wieland, F. Allgöwer, Constructive safety using control barrier functions, IFAC Proc. Vol. 40 (12) (2007) 462–467.
[22] S.-C. Hsu, X. Xu, A.D. Ames, Control barrier function based quadratic programs with application to bipedal robotic walking, in: 2015 American Control Conference, ACC, IEEE, 2015, pp. 4542–4548.
[23] W. Xiao, C. Belta, High-order control barrier functions, IEEE Trans. Automat. Control 67 (7) (2022) 3655–3662.
[24] W. Xiao, C.A. Belta, C.G. Cassandras, Sufficient conditions for feasibility of optimal control problems using control barrier functions, Automatica 135 (2022) 109960.
[25] K.P. Tee, S.S. Ge, E.H. Tay, Barrier Lyapunov functions for the control of output-constrained nonlinear systems, Automatica 45 (4) (2009) 918–927.
[26] T.G. Molnár, A.W. Singletary, G. Orosz, A.D. Ames, Safety-critical control of compartmental epidemiological models with measurement delays, IEEE Control Syst. Lett. 5 (5) (2021) 1537–1542.
[27] B.A. Butler, P.E. Paré, Optimal safety-critical control of epidemics, IEEE Control Syst. Lett. (2023).
[28] S.A. Rosenberg, N.P. Restifo, J.C. Yang, R.A. Morgan, M.E. Dudley, Adoptive cell transfer: a clinical path to effective cancer immunotherapy, Nat. Rev. Cancer 8 (4) (2008) 299–308.
[29] A.D. Ames, S. Coogan, M. Egerstedt, G. Notomista, K. Sreenath, P. Tabuada, Control barrier functions: Theory and applications, in: 2019 18th European Control Conference, ECC, IEEE, 2019, pp. 3420–3431.
[30] Q. Nguyen, K. Sreenath, Exponential control barrier functions for enforcing high relative-degree safety-critical constraints, in: 2016 American Control Conference, ACC, IEEE, 2016, pp. 322–328.
[31] J. Koenemann, G. Licitra, M. Alp, M. Diehl, Openocl–open optimal control library.